Electronic Supplementary Information

Ultrathin MnO_2 Nanoflakes as an Efficient Catalyst for Oxygen Reduction Reaction

Chao Wei,[a,b] Linghui Yu,[a] Chenlong Cui,[a] Jiadan Lin,[c] Chen Wei,[c] Nripan Mathews,[a,d,e] Fengwei Huo,[a] Thirumany Sritharan,[a,e] Zhichuan Xu[a,b,d]*

[a] School of Materials Science and Engineering, Nanyang Technological University, 50 Nanyang Avenue, Singapore 639798, Singapore; [b] Solar Fuels Lab, Nanyang Technological University, 50 Nanyang Avenue, Singapore 639798, Singapore; [c] Department of Physics, National University of Singapore, 3 Science Drive 3, Singapore 117543; [d] Energy Research Institute @ NTU, Nanyang Technological University, 50 Nanyang Avenue, Singapore 639798, Singapore; [e] Singapore-Berkeley Research Initiative for Sustainable Energy, 1 Create Way, 138602 Singapore.

*Corresponding Author: xuzc@ntu.edu.sg

Experimental Details

Synthesis of MnO_2 nanoflakes. MnO_2 nanoflakes were synthesized in aqueous solution through a typical hot-injection method: pre-dissolved potassium permanganate ($KMnO_4$) solution was quickly added into hexadecyltrimethylammonium bromide (CTAB) solution at 140 ^oC, giving a mixture containing 0.05 M CTAB and 0.01 M $KMnO_4$. Temperature of oil bath was maintained at 140 ^oC. MnO_2 was collected by adding acetone and following centrifugation. The molar ratio of CTAB/$KMnO_4$ was varied as control experiments.

Carbon loading. A suspension solution of carbon nanotube (~0.5 mg/ml) was prepared by sonicating the carbon nanotube in ethanol for 3 hours. Afterwards, a solution of as-synthesized MnO_2 NPs (dispersed in ethanol) was added drop-wise into the carbon solution and the mixture was further sonicated for 2 hours. The MnO_2/C precipitation was collected by centrifuging for 10 min at 9500 rpm and was subsequently dried at 80 ^oC for further use. In order to ensure the mass loading of MnO_2 to be 20 wt%, the concentration of MnO_2 NPs solution used in carbon loading was determined by inductively coupled plasma-atomic emission spectroscopy (ICP-AES).

Electrode preparation. Typically, as-prepared MnO_2/C was dispersed in a mixture of solvents containing water, isopropanol and Nafion® perfluorinated resin solution (5 wt% in water) (v/v/v = 4/1/0.05) by sonication for 30 min to form a 2 mg/mL suspension. 15 μL of this ink was then dropped onto the rotating disk electrode (RDE, 0.196 cm^2, PINE) and dried at room temperature, yielding a MnO_2 mass loading of 6 μg (30.6 μg $cm^{-2}{}_{disk}$). As a control experiment, commercial

Pt/C (50 wt%) was dispersed in the same mixture solvents to form a 0.8 mg/mL suspension. 15 µL of this ink was then dropped onto the RDE and dried at room temperature, yielding a Pt mass loading of 6 µg (30.6 µg $\mathrm{cm^{-2}}_{\mathrm{disk}}$).

Electrochemical characterization (ORR). Electrochemical measurements were conducted with a rotating-disk electrode (Pine) using a PINE WaveDriver 20 bipotentiostat. The 0.1 M KOH electrolyte was prepared from Milli-Q water (18 MΩ·cm) and KOH pellets (99.99% weight, Sigma-Aldrich). All electrochemical results were collected in a three-electrode glass cell and potentials were referenced to RHE scale. To avoid impurities from the corrosion of the glass cell, all experiment data was collected within 2 hr since the initial exposure of electrolyte to the glass cell. ORR activities were obtained from the 10 mV/s positive-going scans in O_2 saturation at 1600 rpm and were corrected for capacitive currents in Ar saturation. The mass transport correction was performed employing the well-known Levich equation

$$i_{\mathrm{measured}}{}^{-1} = i_{\mathrm{k}}{}^{-1} + i_{\mathrm{D}}{}^{-1}$$

where i_{measured} is the measured O_2 reduction current density, i_{k} is the mass-transport-corrected kinetic ORR current density, and i_{D} represents the limiting current density. The number of electron (n) transferred was estimated according to the Koutecky-Levich analysis, where the slope of the lines is related to n exchanged in the overall ORR

$$\mathrm{slope} = (0.62nFD_{\mathrm{o}}^{2/3}\upsilon^{-1/6}C_{\mathrm{o}})^{-1}$$

where F is Faraday's constant, D_{o} is the diffusivity of O_2 molecule in the electrolyte, ω is the rotation speed, υ is the kinetic viscosity, and C_{o} is the concentration of O_2 in the electrolyte.[1]

iR-correction (impedance measurement). The resistance of electrolyte was measured right after the ORR CV measurements at a constant potential with a 10 mV voltage perturbation applied. The ac spectra were collected from 200 kHz to 1 Hz, where the real part of the resistance at 1 kHz was used as the solution resistance (45 Ω, this work).[2] The ORR polarization curves were then corrected to obtain iR-free potential (E - iR) of the working electrode.

Determination of catalyst surface area. The electrochemical surface area (ESA) measurements of commercial Pt/C (50 wt%) were performed in Ar-saturated 0.1 M KOH solution. The CV was scanned from 0.03 V to 1.1 V vs. RHE at a sweep rate of 50 mV/s The hydrogen adsorption/desorption region from 0.05 V to ~0.4 V vs. RHE was integrated and averaged to calculate the Pt surface area, assuming a charge density of 210 $\mu\mathrm{C/cm^2}_{\mathrm{Pt}}$ for one monolayer of hydrogen coverage.[2,3] The ESA of the commercial Pt/C (50 wt%) in this work was estimated to be 21.7 ± 0.9 $\mathrm{m^2/g}$. The surface area of MnO_2 is determined by BET measurement.

TEM characterization and size analysis. ~2 µl water solution of MnO_2 nanoflakes was dropped onto amorphous carbon coated TEM Cu grid and allowed to dry at room temperature. The TEM images are recorded on a JEOL 2010 TEM at 200 kV. The number-average width W_n, was calculated as follows:

$$dW_n = \frac{\sum_{i=1}^{n} dW_i}{n}$$

where W_i is the width of individual flakes, n is the number of counted unfolded flakes. W_i was determined by averaging the width measured at two different directions that are perpendicular to each other.

X-ray diffraction (XRD). XRD samples were prepared by dropping highly concentrated sample suspensions onto glass slides. XRD patterns were collected by Shimadzu (thin film) with a Cu Kα radiation (λ = 1.5418 Å).

X-ray Photoelectron Spectroscopy (XPS). The manganese oxidation state of as-synthesized MnO_2 was determined from the Mn 3s and O 1s core level spectra, which were measured by a Kratos AXIS Ultra Imaging X-ray photoelectron spectrometer (XPS).

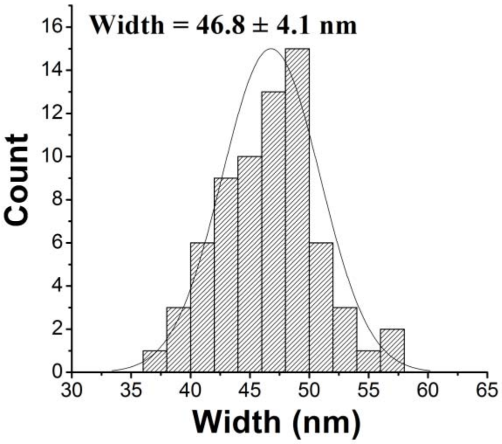

Figure S1. The size distribution histogram of nanoflakes by measuring over 150 unfolded flakes under TEM.

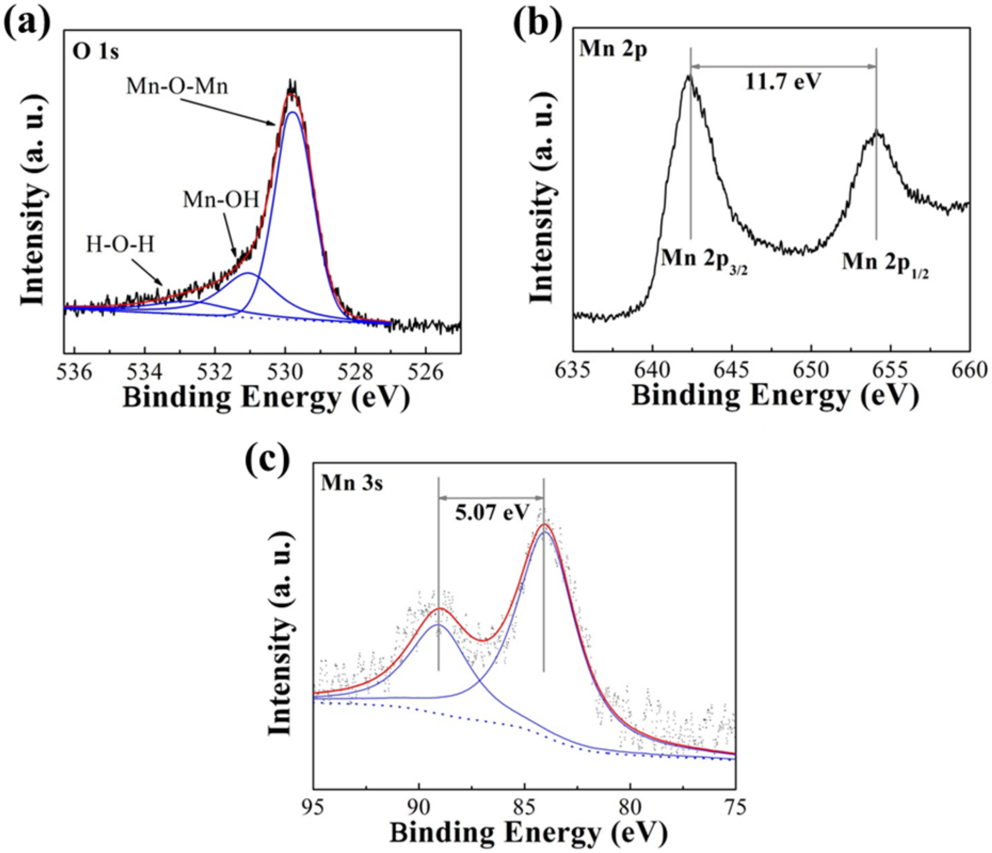

Figure S2. XPS survey spectra of O 1s (a), Mn 2p (b) and Mn 3s (c). The Mn 2p spectra (Figure) shows the energy separation between Mn $2p_{3/2}$ (654.1 eV) and Mn $2p_{1/2}$ (642.4 eV) is 11.7 eV, which is in agreement with the previous reports[4-6]. Chigane *et al*[5] had demonstrated the linear relationship between the energy separation of the Mn 3s peaks and Mn oxidation state of manganese oxides, where Mn^{4+} and Mn^{3+} oxides should have a peak gap of about 4.7 and 5.4 eV, respectively. According to this relationship, the as-prepared MnO_2 nanoflakes show separation energy of of 5.07 eV (Figure), suggesting the Mn oxidation state is 3.47. Moreover, based on the O 1s spectra, the average manganese oxidation state was computed from the intensities of the Mn-O-Mn and Mn-OH components according to

$$Oxidation\ State = \frac{4 \times (S_{Mn-O-Mn} - S_{Mn-OH}) + 3 \times S_{Mn-OH}}{S_{Mn-O-Mn}}$$

where *S* refers to the peak area of different components of O 1s spectra.[6] The calculation result is 3.58.

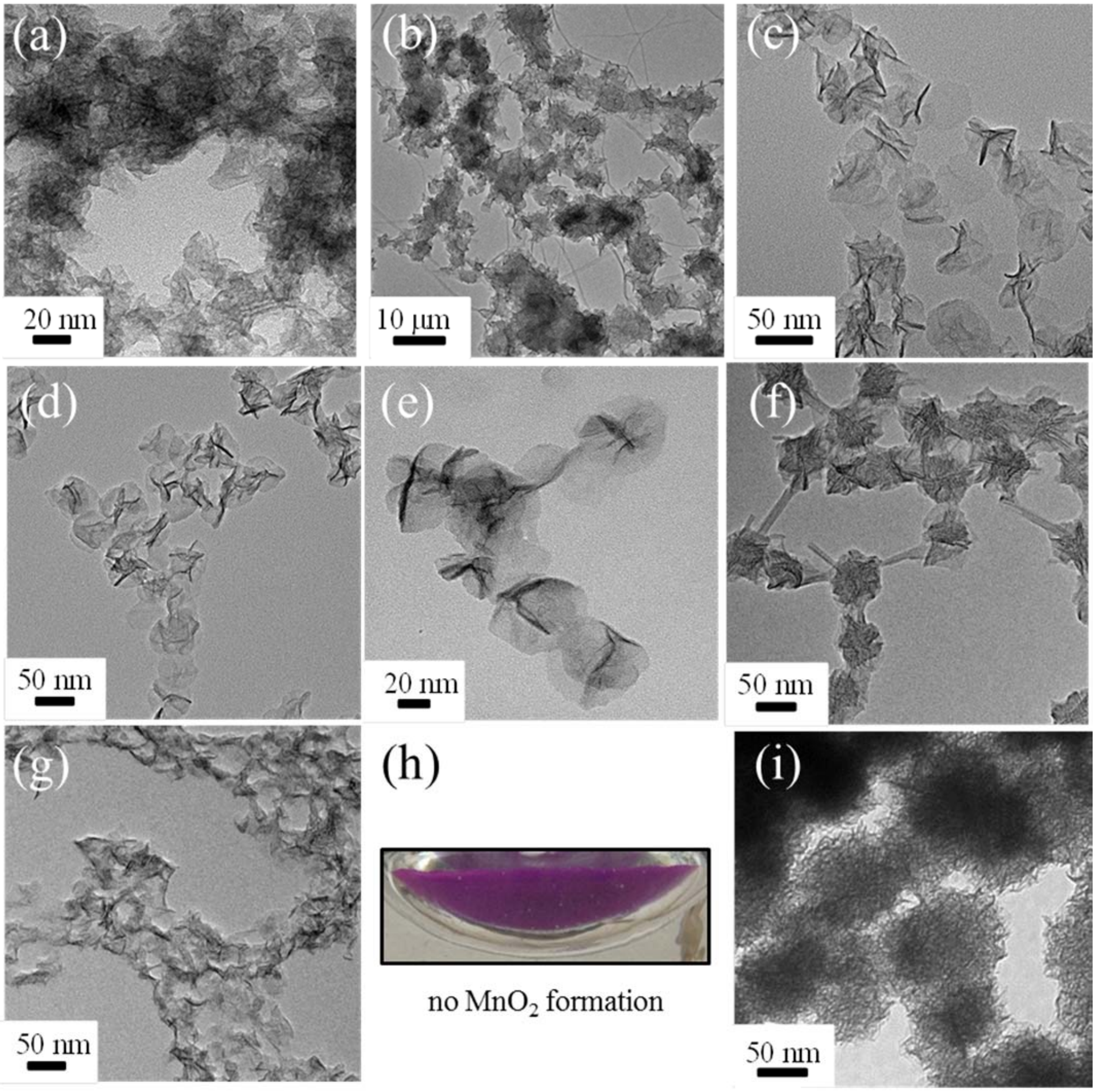

Figure S3. The representative TEM images of a series of control experiments. The corresponding recipes are indicated in the table below.

S/N	$KMnO_4$	CTAB	Method
a	0.1 M	0.05 M	Hot-injection
b	0.05 M	0.05 M	Hot-injection
c	0.02 M	0.05 M	Hot-injection
d	0.01 M	0.05 M	Hot-injection
e	0.005 M	0.05 M	Hot-injection
f	0.01 M	0.05 M	Heating-up
g		0.05 M (CTAC)	Hot-injection
h		0.05 M (KBr)	Hot-injection
i		0.05 M (SDS)	Hot-injection

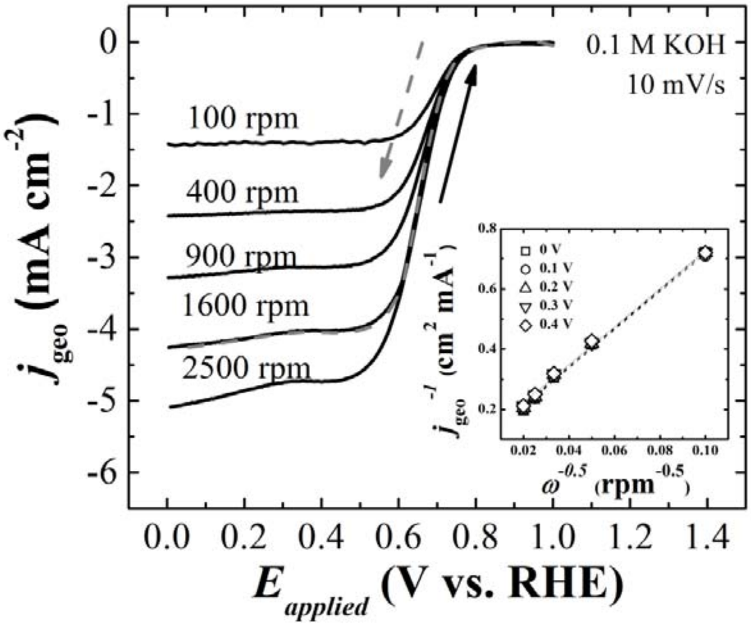

Figure S5. ORR current densities (capacity-corrected positive-going scans) of large MnO_2 particles collected at 10 mV/s. The rotation rates are 100, 400, 900, 1600, 2500 rpm. The specific activity and mass activity were obtained by three independent measurements. Solid lines represent positive-going scans and only negative-going scans at 1600 rpm are shown by the dash lines. The inset shows the Koutecky-Levich plots at 0, 0.1, 0.2, 0.3, and 0.4 V (vs. RHE).

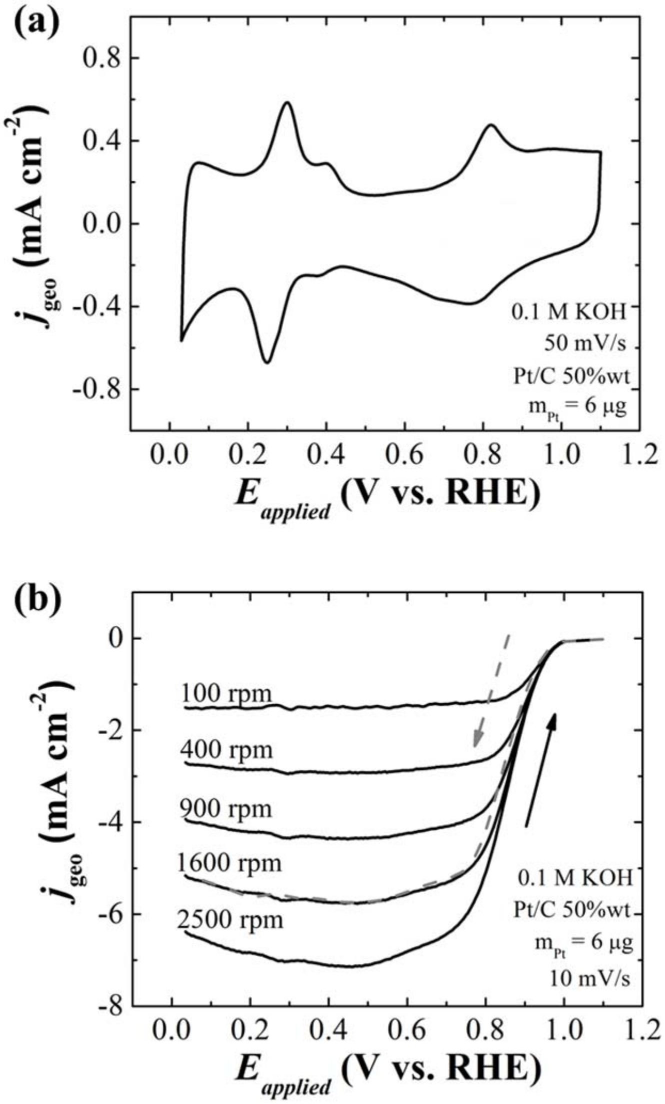

Figure S6. (a) CVs of commercial Pt/C (50 wt%) at 50 mV/s in at room temperature in Ar-saturated 0.1 M KOH. (b) ORR current densities (capacity-corrected positive-going scans) collected at 10 mV/s. The rotation rates are 100, 400, 900, 1600, 2500 rpm. The specific activity and mass activity were obtained by three independent measurements. Solid lines represent positive-going scans and only negative-going scans at 1600 rpm are shown by the dash lines.

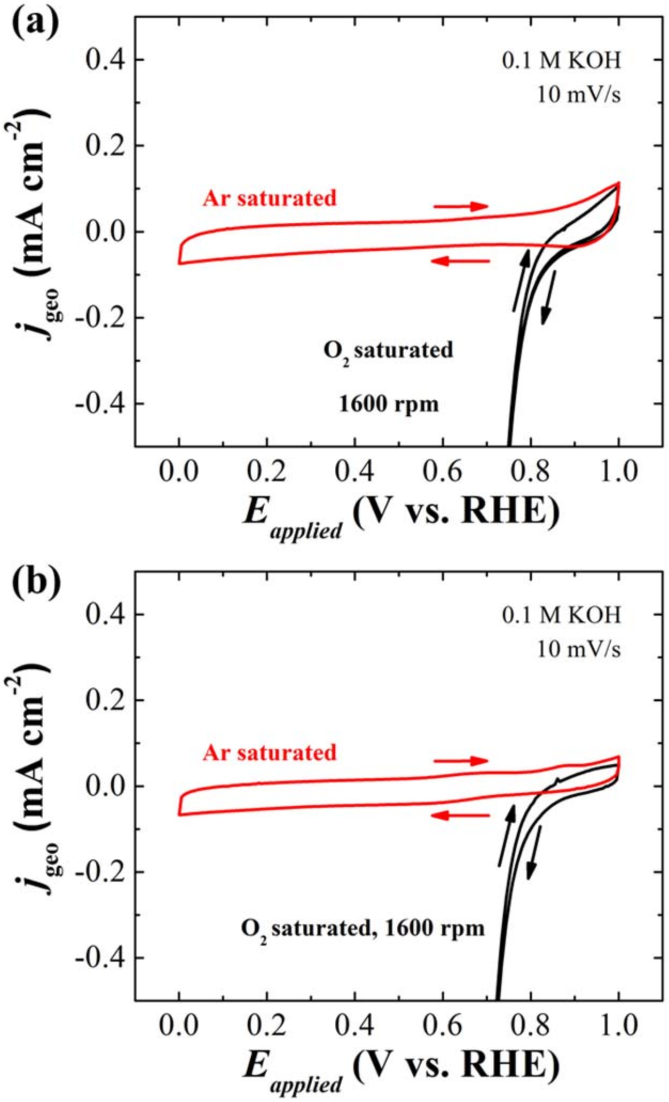

Figure S7. CVs of (a) MnO_2 nanoflakes and (b) large particles at 10 mV/s in 0.1 M KOH at room temperature in Ar-saturated electrolyte at 0 rpm.

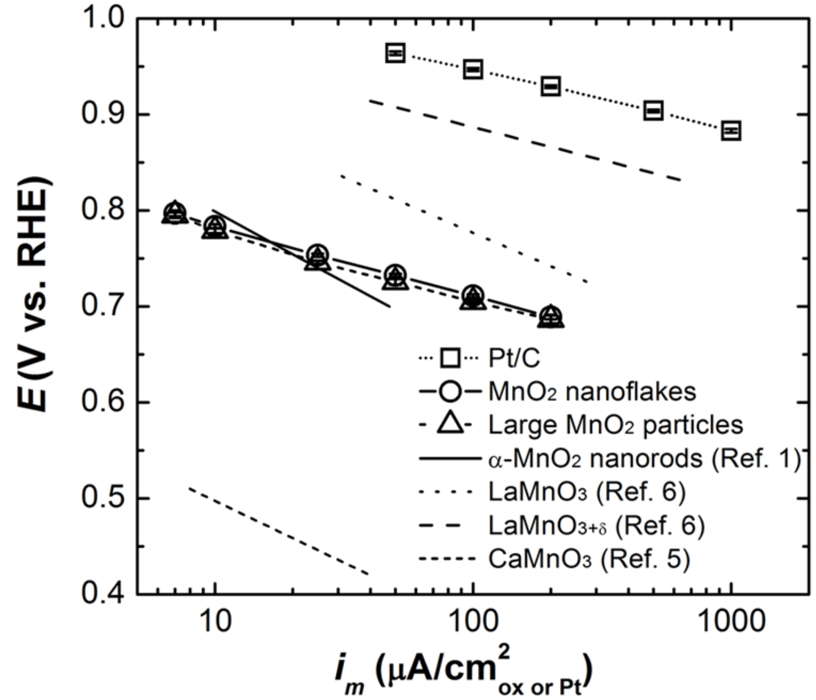

Figure S8. Specific activities of MnO_2 nanoflakes, large particles, and commercial Pt/C. For comparison, α-MnO_2 nanorods,[1] $CaMnO_3$,[7] $LaMnO_3$,[8] and $LaMnO_{3+\delta}$ [8] are calculated and read from reported literatures. Error bar represents for at least three independent experiments.

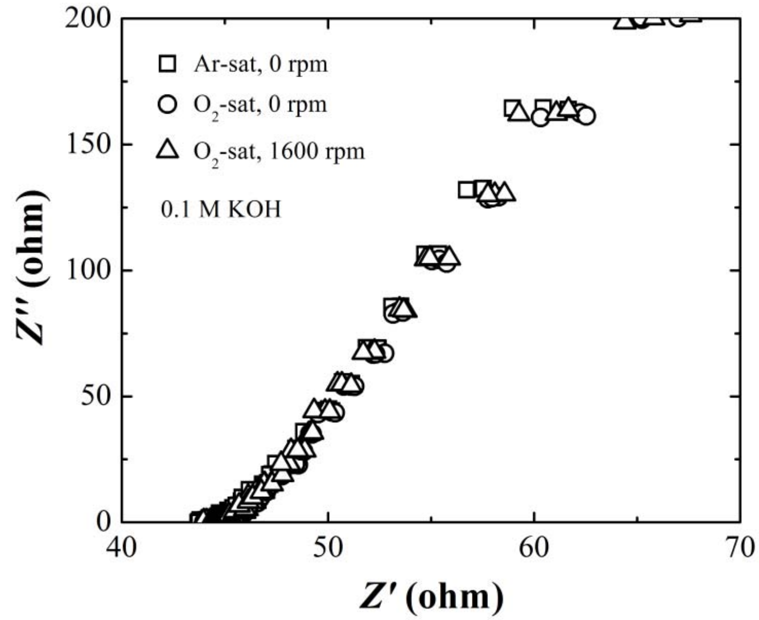

Figure S9. Electrochemical impedance spectra of electrolyte (0.1 M KOH) resistance under different conditions.

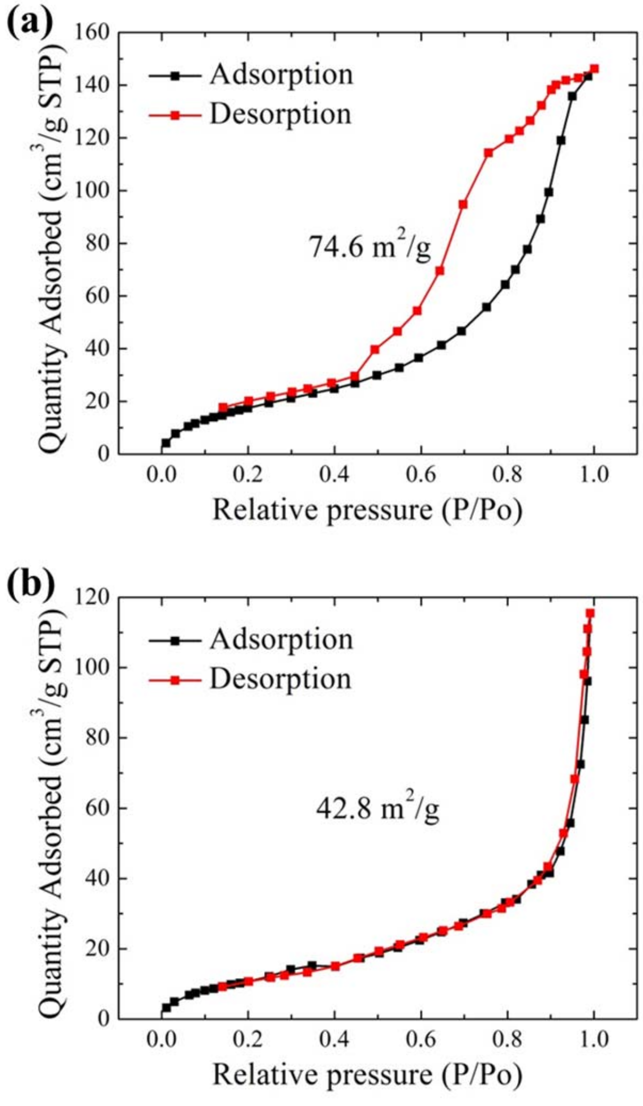

Figure S10. BET measurement of (a) as-synthesized MnO_2 nanoflakes and (b) MnO_2 large particles.

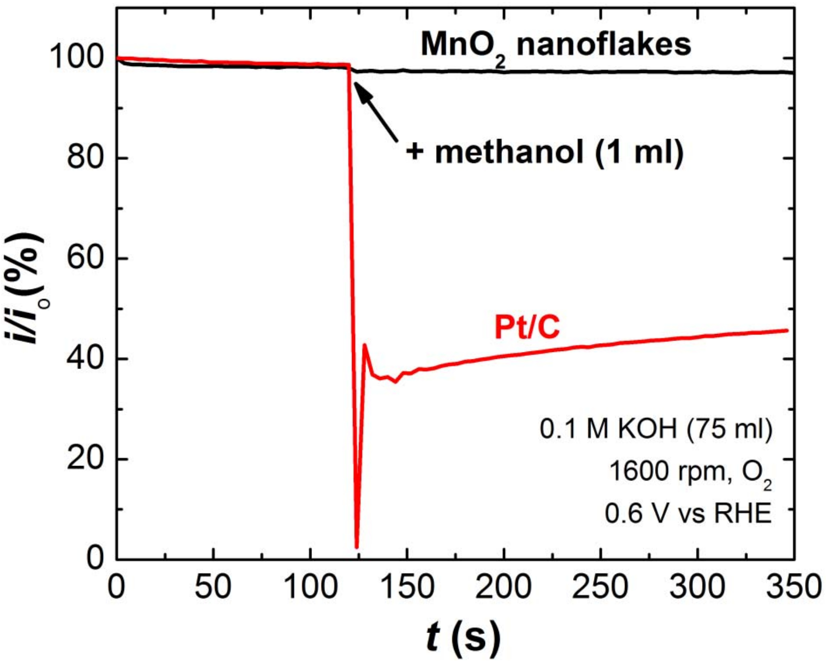

Figure S11. Chronoamperometric response of as-synthesized MnO_2 nanoflakes and Pt/C at 0.6 V vs. RHE with a rotation speed of 1600 rpm. Methanol crossover was tested by injecting 1 ml methanol into 75 ml O_2-saturated 0.1 M KOH electrolyte.

Table S1. Summary of specific and mass activities of reference catalysts at 0.75 V vs. RHE. Mass activity (i_m) of B-doped CNT,[9] $LaMnO_3$,[8] α-MnO_2 nanorods,[1] β-MnO_2,[10] and N-doped graphene[11] were calculated based on the available experiment details provided in the literature. Mass activity of MnO_2 (J.E.C)[12] was directly read. Specific activity (i_s) of $LaMnO_3$[8] was read and specific activity of α-MnO_2 nanorods[1] was calculated. All reference data was converted to RHE scale according to the reported electrolyte and reference electrodes. The blank indicates that the information is not available in the corresponding papers.

Catalyst	B-doped CNT	$LaMnO_3$	α-MnO_2 (rod)	β-MnO_2	MnO_2 (J.E.S)	N-doped graphene
References #	9	8	1	10	12	11
$i_{measued}$ (mA/cm^2)			1.1	0.2		0.1
$I_{measued}$ (mA)	0.09					
i_d (mA/cm^2)			3.1	5.5		0.8
I_d (mA)	0.42					
A_{RDE} (cm^2)			0.1256	0.196		0.196
$m_{catalys}$ (µg)	20		40	20		7.5
A_s (m^2/g)		0.6	25			
Electrolyte	1 M NaOH	0.1 M KOH	0.1 M KOH	0.1 M KOH	1 M KOH	0.1 M KOH
Reference electrode	SCE			Hg/HgO	Hg/HgO	Ag/AgCl (4 M KCl)
Conversion factor (V vs. RHE)	1.06			0.87		0.96
i_m (mA/mg)	6.67	1.2	5.35	2	3.7	3
i_s (µA/cm^2)		200	21.4			

Reference

(1) Xiao, W.; Wang, D.; Lou, X. W. *The Journal of Physical Chemistry C* **2009**, *114*, 1694.
(2) Sheng, W.; Myint, M.; Chen, J. G.; Yan, Y. *Energy & Environmental Science* **2013**, *6*, 1509.
(3) Suntivich, J.; Xu, Z.; Carlton, C. E.; Kim, J.; Han, B.; Lee, S. W.; Bonnet, N.; Marzari, N.; Allard, L. F.; Gasteiger, H. A.; Hamad-Schifferli, K.; Shao-Horn, Y. *J Am Chem Soc* **2013**, *135*, 7985.
(4) Lee, S. W.; Kim, J.; Chen, S.; Hammond, P. T.; Shao-Horn, Y. *ACS Nano* **2010**, *4*, 3889.
(5) Chigane, M.; Ishikawa, M. *Journal of The Electrochemical Society* **2000**, *147*, 2246.
(6) Toupin, M.; Brousse, T.; Bélanger, D. *Chemistry of Materials* **2004**, *16*, 3184.
(7) Stoerzinger, K. A.; Risch, M.; Suntivich, J.; Lu, W. M.; Zhou, J.; Biegalski, M. D.; Christen, H. M.; Ariando; Venkatesan, T.; Shao-Horn, Y. *Energy & Environmental Science* **2013**, *6*, 1582.
(8) Suntivich, J.; Gasteiger, H. A.; Yabuuchi, N.; Nakanishi, H.; Goodenough, J. B.; Shao-Horn, Y. *Nature chemistry* **2011**, *3*, 546.
(9) Yang, L.; Jiang, S.; Zhao, Y.; Zhu, L.; Chen, S.; Wang, X.; Wu, Q.; Ma, J.; Ma, Y.; Hu, Z. *Angewandte Chemie International Edition* **2011**, *50*, 7132.
(10) Sun, W.; Hsu, A.; Chen, R. *Journal of Power Sources* **2011**, *196*, 4491.
(11) Qu, L. T.; Liu, Y.; Baek, J. B.; Dai, L. M. *Acs Nano* **2010**, *4*, 1321.
(12) Lima, F. H. B.; Calegaro, M. L.; Ticianelli, E. A. *Journal of Electroanalytical Chemistry* **2006**, *590*, 152.